Rate-Splitting Multiple Access for Indoor Visible Light Communication Networks

Shimaa A. Naser
Khalifa University
Abu Dhabi, UAE
shimaa.naser@ku.ac.ae

Paschalis C. Sofotasios
Khalifa University, UAE
Tampere University, Finland
p.sofotasios@ieee.org

Sami Muhaidat
Khalifa University, UAE
Carleton University, Canada
muhaidat@ieee.org

Mahmoud Al-Qutayri
Khalifa University
Abu Dhabi, UAE
mahmoud.alqutayri@ku.ac.ae

***Abstract*—Visible light communication (VLC) has been emerged as a technology that can increase the channel capacity in the next generations of wireless technologies by exploiting the largely unutilized, licence-free and huge visible light portion of the electromagnetic spectrum. In order to enable high-speed short-range wireless communications, VLC utilizes the installed high-switching rate light emitting diodes (LEDs) in the ceilings of indoor environments, which are primarily used for illumination, to modulate the signals into visible light intensity. However, VLC suffers from several limitations, such as the limited modulation bandwidth and the coverage area of LEDs that degrade the overall system spectral efficiency (SE). In this respect, the present contribution proposes rate splitting multiple access (RSMA) for multi-cell indoor VLC systems as a mean to enhance the overall system SE and energy efficiency (EE) as well as to provide ubiquitous indoor coverage and to address user mobility issues. Moreover, we utilize coordinated beamforming to design the precoders of the common and the private streams in each cell aiming to enhance the performance of cell-edge users. Finally, the formulated sum of the mean squared error optimization problem is solved sub-optimally using an alternating optimization approach. Extensive computer simulations demonstrate that RSMA improves the overall system performance in terms of the SE and EE compared to the recently used multiple access techniques, such as space division multiple access with coordinated beamforming which constitutes a special case of it.**

I. INTRODUCTION

Wireless spectrum resources are particularly scarce since most of the frequency bands are already occupied. However, the visible light portion of the electromagnetic spectrum is still not exploited and can be used without any licensing. This has motivated the emergence of visible light communication (VLC) to complement the congested RF-based wireless systems [1]. It is recalled that VLC is realized by using light emitting diodes (LEDs) in recent infrastructures, which are primarily used for illumination, to modulate the signals into the light intensity, which is known as intensity modulation (IM). On the contrary, at the receiver side a photo-detector (PD) is used to convert light into an electrical signal for detection, a process known as direct detection (DD) [2]–[11].

Compared to RF, VLC systems are characterized by high security, high degree of spatial reuse, and immunity to electromagnetic interference. However, their performance is highly affected by several factors, such as the limited modulation bandwidth of LEDs as well as the restrictions imposed by IM/DD, which require signals to be positive and real-valued [12]. Motivated by this, several efficient optical-based modulation and coding schemes, multiple-input multiple-output (MIMO) schemes, VLC cooperative communications, and multiple access (MA) schemes have been proposed in the open technical literature, aiming to enhance the achievable spectral efficiency (SE) of VLC systems [13]–[15].

Typically, the channel of a VLC link is considered to be line-of-sight (LoS), with the non-line-of-sight components typically neglected. Therefore, ensuring that a link is available at all times as well as the provision of wider coverage area and the support of users mobility are of paramount importance [3]. In recent large rooms/offices, uniform illumination is guaranteed though the deployment of multiple wide-beam illuminating devices, which introduced the concept of optical attocells. In each attocell, an LED array acts as a VLC access point (VLC-AP) that is capable of handling multiple user equipment (UE) devices located in its coverage area. In such multi-cell systems, the received signals at cell-edge users are corrupted by interference from signals of the users within the same cell, known as intra-cell interference i.e., inter-user interference (IUI), and from signals of users in the adjacent cells known as inter-cell interference (ICI).

In general, it is difficult to handle the interference at UEs side due to lack of coordination among them. As a result, interference mitigation should be performed before transmission at the transmitters side. Hence, in order to improve the performance of the cell-edge users, different time, frequency, or power allocation coordination schemes across the involved attocells have been investigated [16]–[18]. Examples of theses schemes include: multi-color schemes [19], multicarrier-based cell partitioning [20], optimized angle diversity receivers [21], and differential optical detection. Yet, even though the aforementioned techniques have showed an improvement on the achievable SE compared to the single cell case, they typically require dedicated receiver/transmitter architectures [22].

In large-scale VLC networks, it is common that a VLC-AP has multiple LED arrays that are connected through backbone links to mimic a MIMO configuration. Therefore, precoding techniques are efficient in mitigating or eliminating ICI by appropriately weighing the messages for different users at the LEDs input. In the context of multi-cell MIMO VLC systems, different VLC-APs are interconnected through backbone links in order to provide a certain level of coordination/cooperation

among them [23]. Coordinated beamforming (CB) (one kind of coordinated multi-point techniques) has been recently proposed as a compromise solution in terms of complexity and performance compared to joint transmission and per-cell coordination. In CB, only channel state information (CSI) is shared between cells, and the precoders design at different cells is performed in a coordinated way [24].

It is recalled that power-domain non-orthogonal multiple access (NOMA) has been also studied in the context of multi-cell VLC. To this end, despite the SE gain offered by NOMA, its performance is highly degraded due the channel correlation in VLC systems. Additionally, the complexity and the error propagation issues become more severe as the number of users in the system is very large, which is attributed to increased number of the required successive interference cancellation (SIC) layers at the receivers. In order to alleviate these limitations in the multi-cell VLC context, different approaches have been explored in the literature. In [25], [26], the authors proposed location-based user grouping and communications scheduling in order to reduce ICI. Even though this method is interesting, it in turn resulted in a high data overhead. Alternatively, [27] combined offset quadrature-amplitude-modulation/orthogonal frequency division multiplexing (QAM/OFDM) with NOMA for asynchronous multi-cell communications. It was shown that this technique outperforms the benchmark "combined OFDM and NOMA" in terms of capacity and flexibility. Moreover, [28] proposed a hybrid NOMA-zero-forcing (NOMA-ZF) approach, where the VLC-AP serves cell-centered UEs using NOMA, but communicates with cell-edge UEs through ZF. Finally, authors of [29] proposed a hybrid time scheduling-NOMA, where location-based grouped UEs within a cell are served in different time slots, in order to reduce ICI.

Recently, Rate Splitting Multiple Access (RSMA) emerged as a robust and generalized MA scheme for future wireless systems, able to accommodate different users in a heterogeneous environment [30]–[32]. It has been shown in MIMO-based RF systems that RSMA outperforms and generalizes other MA schemes such as NOMA and space division multiple access (SDMA), in terms of both SE and energy efficiency (EE) [33], [34]. To achieve this, messages of all users are divided into one or several common parts, and a private part. Subsequently, all common parts are multiplexed and encoded into a single (or several) common streams intended for all (or to a subset of) users. Also, the private parts are encoded separately into multiple private streams, which are then superimposed with the common stream(s). The resulted super-symbol is then transmitted to all users over the VLC downlink channel. Then, at each user, the common streams are decoded first in order to obtain the common parts of the intended user, utilizing iterative SIC. Subsequently, the private part is decoded while treating the other users' private parts as noise.

In multi-cell VLC systems, RSMA is deemed to bring several advantages. Through its precoding flexibility, it can mitigate efficiently the incurred interference, hence achieving higher SE performances. Moreover, unlike NOMA VLC networks that require multi-layer SIC receivers, single-layer RSMA with only one common message is expected to achieve better SE using only one SIC layer at the receivers. Hence, the RSMA VLC framework is less complex compared to NOMA based frameworks. Of note, the splitting of the messages into common and private parts enables RSMA to provide robust services for different network loads and users' deployments. With this motivation, this contribution proposes one-layer RSMA for indoor multi-cell VLC systems. Additionally, we exploit CB to design the precoders for the common and private streams, aiming to minimize the sum of the mean squared error (MSE) across all users. The proposed system model is expected to provide useful insights on the use of RSMA in VLC systems. Specifically, it is shown that it can efficiently mitigate the ICI at cell-edge users, enhance the overall system SE and EE, and adapt to different UEs' deployment scenarios.

To the best of the authors' knowledge, such a study has not been previously reported in the open technical literature. The remainder of the paper is organized as follows: In section II, preliminary information about single-cell configuration is presented and two special cases for RSMA are explained. Then, section III presents the main contribution which is RSMA in multi-cell VLC system. Section IV illustrates and discusses the simulation results. Finally, Section V concludes the paper with some useful remarks.

Notations: Throughout the paper, boldface uppercase and lowercase represent matrices and vectors, respectively. $(\cdot)^T$ denotes the transpose operation. $\mathbb{E}(\cdot)$ is the statistical expectation, $||\cdot||$ is the Euclidean norm, and $|\cdot|$ is the absolute value. Also, assuming a vector $\mathbf{z} = [z_1, \cdots, z_Z]$ with length Z, $L_1(\mathbf{z}) = \sum_{i=1}^{Z} |z_i|$ denotes the L_1 norm. Finally, $\mathbf{1}_{N\times 1}$ is the all-ones vector of size $N \times 1$ and $\boldsymbol{I}$ is the identity matrix.

II. RSMA FOR VLC

In this section we firstly consider preliminary information about the implementation of RSMA in single-cell VLC systems for a simple two-user model. Then, we illustrate how SDMA and NOMA can be considered special cases of RSMA.

A. RSMA in single-cell configurations

For simplicity, we consider a simple case in Fig.1, where we assume that two transmitting LEDs are connected to a central processing unit and send messages to two single-PD users in a single cell scenario [14]. The principle of RSMA is described as follows: messages of all users are divided into two different parts, one common between all users and one private which is intended only for the associated user. In our two-user model, U_1 is divided into the private part U_1^1 and the common part U_1^{12}. Similarly, U_2 is divided into the private part U_2^2 and the common part U_2^{12}. Then, the two private messages, U_1^1 and U_2^2, are encoded into distinct private streams s_1 and s_2, respectively. Then, from a common codebook, U_1^{12} and U_2^{12} are multiplexed and encoded into a common stream s_{12} that will be decoded by both users, which are equipped with SIC for interference mitigation. Furthermore, we assume that s_i ($i \in \{1, 2, 12\}$) is randomly selected from a pulse amplitude modulation constellation also with zero mean and normalized

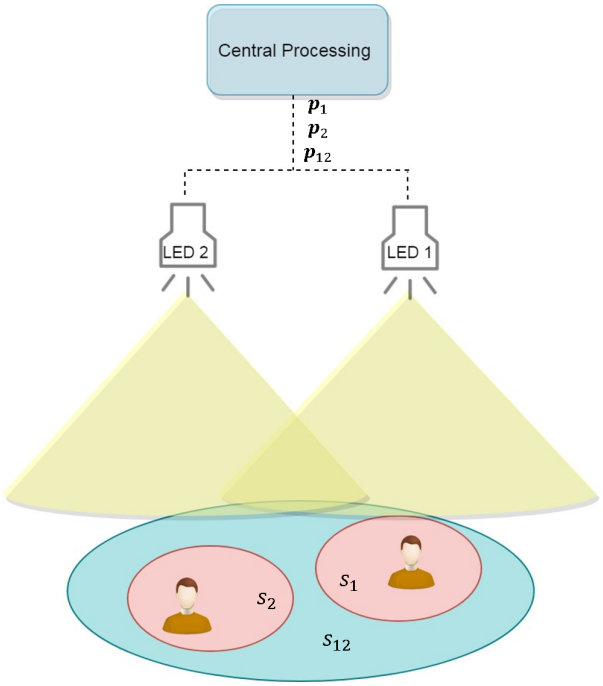

Fig. 1. System model for single-cell two RSMA users

range $\{-1, 1\}$. Therefore, the vector of the transmitted streams is denoted by $\mathbf{s} = [s_1, s_2, s_{12}]^T$, where $\mathbb{E}(\mathbf{s}\mathbf{s}^T) = \mathbf{I}$. To reduce multi-user interference (MUI), a linear precoding matrix $\mathbf{P} = [\mathbf{p}_1, \mathbf{p}_2, \mathbf{p}_{12}]$ is considered, where $\mathbf{p}_i = [p_{i,1}\, p_{i,2}]^T \in \mathbb{R}_{2\times 1}$ is the precoding vector for the i^{th} stream. A direct current (DC) bias $\mathbf{I}^{DC} \in \mathbb{R}_{2\times 1}$ is added in order to ensure positive signals at the LEDs input. Hence, the transmitted signal, $\mathbf{x} \in \mathbb{R}^{+}_{2\times 1}$, can be written as [14]

$$\mathbf{x} = [x_1, x_2]^T = \mathbf{P}\mathbf{s} + \mathbf{I}^{DC} = \sum_{i\in\{1,2,12\}} \mathbf{p}_i s_i + \mathbf{I}^{DC} \tag{1}$$

and the received signal at the k^{th} PD, after optical-to-electrical conversion, is expressed as

$$y_k = \varsigma\zeta \mathbf{h}_k^T \mathbf{x} + n_k,\ \forall k \in \{1, 2\} \tag{2}$$

where ς is the conversion factor of any LED chip in the LED array (consists of N_b LED chips), ζ is the responsivity of any PD, $\mathbf{h}_k = [h_{k,1}, h_{k,2}]^T$ is the DC channel gain vector between the k^{th} PD and the transmitting LEDs, where each element is expressed as follows [14]

$$h = \begin{cases} \frac{AN_b}{r^2} R_o(\varphi) T_s(\phi) g(\phi) \cos(\phi), & 0 \leqslant \phi \leqslant \phi_c \\ 0, & \text{otherwise,} \end{cases} \tag{3}$$

where A denotes the UE's PD area, N_b is the number of LED chips per LED array, and r is the distance between a LED array and a UE. Moreover, φ is the transmission angle from a LED to a UE, ϕ denotes the incident angle with respect to the receiver, and ϕ_c is the field of view (FoV) of the PD. Finally, $T_s(\phi)$ is the gain of the optical filter, and $g(\phi)$ is the gain of the optical concentrator which can be calculated based on [2]. Moreover, $n_k \sim \mathcal{N}(0, \sigma_k^2)$ is the additive white Gaussian noise, representing the thermal and shot noises, with zero-mean and variance σ_k^2, which can be calculated based on [35]. Due to the low mobility of indoor users, we assume that the channel gains are constant during the transmission, and that perfect CSI is available at the transmitter. In order to accurately design the precoding matrix $\mathbf{P}$, the following constraints need to be satisfied to ensure that the LEDs work in their dynamic range:

$$\begin{aligned} L_1(p_l) &= \sum_{i\in 1,2,12} |p_{l,i}| \\ &= \min\left(I^{DC} - I_{min}, I_{\max} - I^{DC}\right), \quad \forall l \in \{1, 2\} \end{aligned} \tag{4}$$

where p_l is the l^{th} row of the precoding matrix $\mathbf{P}$. Initially, the DC term is removed using an AC coupler; then, minimum mean squared error (MMSE) equalizers are used to detect all different streams. The decoding process for RSMA users is described as follows: at the k^{th} user, the common stream s_{12} is decoded assuming that the private streams are noise. Hence, the received signal-to-interference-plus-noise ratio (SINR) at the k^{th} user for the common stream is expressed as

$$\gamma_k^{12} = \frac{\left(\mathbf{h}_k^T \mathbf{p}_{12}\right)^2}{\left(\mathbf{h}_k^T \mathbf{p}_1\right)^2 + \left(\mathbf{h}_k^T \mathbf{p}_2\right)^2 + \hat{\sigma}_k^2},\ \forall k \in \{1, 2\} \tag{5}$$

where $\hat{\sigma}_k^2 = \sigma_k^2 / (\varsigma\zeta)^2$ is the normalized received noise power. For the sake of simplicity, we assume that ς, ζ are unity and thus $\hat{\sigma}_k^2 = \sigma_k^2$. The k^{th} user extracts its intended information from the decoded common stream, and then the effect of the common stream is removed from the original received signal using SIC. This allows an improvement of the detection of the private streams. So, each user attempts to decode its private stream s_k, while treating the private stream of the other user as noise. Consequently, the received SINR at the k^{th} user, for its private stream, can be written as

$$\gamma_k^k = \frac{\left(\mathbf{h}_k^T \mathbf{p}_k\right)^2}{\left(\mathbf{h}_k^T \mathbf{p}_{\bar{k}}\right)^2 + \sigma_k^2},\ \forall (k, \bar{k}) \in \{(1, 2), (2, 1)\} \tag{6}$$

and the achieved data rate at user k is expressed by [33],

$$R_k^{12} = \log_2(1 + \gamma_k^{12}), \tag{7}$$

and

$$R_k^k = \log_2(1 + \gamma_k^k),\ \forall k \in \{1, 2\} \tag{8}$$

where R_k^{12} and R_k^k are the data rates for the common and private signals, respectively. In order to ensure successful decoding of the common stream s_{12} at both users, the common rate shall not exceed $R_{12} = \min(R_1^{12}, R_2^{12})$. It is also noted that the targeted common rate for each user can be achieved if R_{12} is adequately shared between the two users, i.e., $R_{12} = \sum_{k=1}^{2} R_{k,\text{com}}$, where $R_{k,\text{com}}$ is the k^{th} user portion of the common rate. Consequently, the total achievable data rate of user k, denoted $R_{k,\text{ov}}$, can be expressed by [33], namely

$$R_{k,\text{ov}} = R_{k,\text{com}} + R_k^k,\ \forall k \in \{1, 2\}. \tag{9}$$

Finally, to design the precoders for the common and the private streams, a formulation of an optimization problem

that maximizes a certain objective function, e.g., sum rate, weighted sum rate (WSR), proportional fairness, or max-min fairness is required. In [14], the maximization of the WSR was adopted as an objective, which is defined as follows assuming that the weights vector for the users $\mathbf{w} = [w_1, w_2]$ are:

$$\max_{\mathbf{P},\mathbf{R}_{\text{com}}} \quad R(\mathbf{w}) = \sum_{k=1}^{2} w_k \, R_{k,\text{ov}} \tag{P1}$$

$$\text{s.t.} \quad L_1(p_l) \leq \varepsilon, \; \forall l \in \{1,2\} \tag{P1.a}$$

$$\sum_{k=1}^{2} R_{k,\text{com}} \leq R_{12} \tag{P1.b}$$

$$\mathbf{R}_{\text{com}} \geq \mathbf{0} \tag{P1.d}$$

where $\mathbf{R}_{\text{com}} = [R_{1,\text{com}}, R_{2,\text{com}}]$ is the common rate vector. Furthermore, P1.a accounts for the optical power constraints associated with the transmitting LEDs. Additionally, to guarantee that the common stream is successfully decoded by both users, constraints P1.b and P1.c were added. To this effect, in [14], it has been shown that (P1) is non-convex due to the presence of variables $\mathbf{p}_k$ ($k \in \{1,2\}$) in the denominator of the SINR expressions (5)-(15). Thus, its solution is not straightforward. Yet, it has been shown in [36] that, WSR maximization problem can be reformulated to an easier problem that minimizes the weighted sum MMSE (WSMMSE). The new reformulated problem jointly optimizes the WMMSE precoding vectors and MSE equalizer weights. Although WSMMSE problem is still non-convex in terms of all the optimization variables, it was shown in [36] that by fixing the values of the precoders, the problem becomes convex in terms of the WMMSE weights and the equalizers gain and vice versa. Thus, a local optimum is guaranteed by utilizing alternating optimization (AO) algorithm. In order to converge to a maximum WSR, the algorithm alternates between updating WMMSE precoding design and MSE equalizer weights design. Further details on the AO procedure are available in Section V.b of [14].

B. Special cases of RSMA

The capability of RSMA to decode part of the interference impeded in the common stream and treat the other users' private messages as a noise allows it to encompass NOMA and SDMA as special cases. It is recalled that in NOMA, users with weak channel conditions are allocated high power coefficients. On the contrary, users with strong channel gains are assigned low power coefficients. Based on this, the weaker user can directly decode its signal while treating the signal of the other users as noise. On the contrary, other users have to remove the interference by decoding the weaker users' signals with the aid of SIC, before detecting its own signal. Thus, NOMA is based on decoding the whole interference from other users' messages, and then cancel it using SIC. Therefore, to obtain NOMA from RSMA, one of the users' messages is encoded into a private stream, i.e., the user with the strongest channel, and the message of the second user is encoded as a common stream. Assuming that user 1 has the strongest channel gain, the transmitted signal can be written as

$$\mathbf{x} = \mathbf{P}\mathbf{s} + \mathbf{d}_{DC} = \sum_{i \in \{1,12\}} \mathbf{p_i} s_i + \mathbf{d}_{DC} \tag{11}$$

and the associated SINRs of the first and second users are

$$\gamma_1^1 = \frac{(\mathbf{h}_1^T \mathbf{p}_1)^2}{\sigma_1^2} \tag{12}$$

and

$$\gamma_2^{12} = \min\left(\frac{(\mathbf{h}_1^T \mathbf{p}_{12})^2}{(\mathbf{h}_1^T \mathbf{p}_1)^2 + \sigma_1^2} \, , \, \frac{(\mathbf{h}_2^T \mathbf{p}_{12})^2}{(\mathbf{h}_2^T \mathbf{p}_1)^2 + \sigma_2^2} \right). \tag{13}$$

On the contrary, SDMA is based on treating any interference from other users' messages as noise. Thus, it can be obtained from RSMA by simply allocating zero power to the common stream. Then, each user's message is encoded only as a private stream. Hence, the transmitted signal in this case is

$$\mathbf{x} = \mathbf{P}\mathbf{s} + \mathbf{d}_{DC} = \sum_{i \in \{1,2\}} \mathbf{p}_i s_i + \mathbf{d}_{DC} \tag{14}$$

and the received SINR at each user simplifies to

$$\gamma_k^k = \frac{\left(\mathbf{h}_k^T \mathbf{p}_k\right)^2}{\left(\mathbf{h}_k^T \mathbf{p}_{\bar{k}}\right)^2 + \sigma_k^2}, \; \forall (k, \bar{k}) \in \{(1,2),(2,1)\}. \tag{15}$$

It was shown in [14] for simple two-user model that RSMA-VLC in single-cell configurations outperforms both NOMA and SDMA in terms of achievable WSR. Also, the effect of channels correlation through considering different users' locations was investigated. It was observed that, NOMA is favored at low signal-to-noise ratio (SNR) for low separation between users, whilst SDMA performs better at high SNRs. On the contrary, RSMA outperformed both NOMA and SDMA and exhibited a robust performance against different users' locations and hence channels correlation. Therefore, RSMA is considered as a particularly suitable MA candidate scheme for VLC in beyond 5G wireless networks.

In the next section, we address the implementation of RSMA in mutli-cell configurations as an efficient way to boost the system SE as well as to provide ubiquitous access in indoor VLC environments, which has not been explored in prior studies. Additionally, the use of CB for the design of the common and private streams is proposed as an effective means for enhancing the performance of cell-edge users.

III. RSMA IN MULTI-CELL CONFIGURATIONS

The single-cell system model in the previous section can be extended to multi-cell configuration for any number of users. To the best of the authors' knowledge, this set up has not been previously investigated in the open literature. Thus, in this section we consider multi-user multi-cell VLC system, composed of N_c attocells, wherein the i^{th} cell is composed of N_l LED arrays and N_u^i single PD users, $\forall i = 1, \ldots, N_c$. The LED arrays in different attocells are interconnected through band-limited backbone links in order to allow designing the

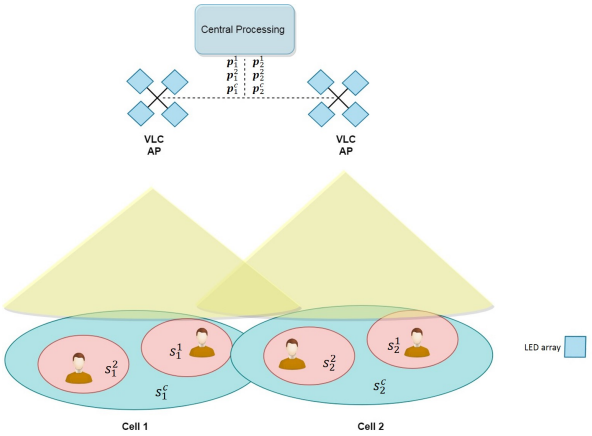

Fig. 2. RSMA in simple multi-cell VLC configuration for $N_c = 2$ and $N_u^i = 2$.

precoders in a coordinated way. A simplified model for $N_c = 2$ and $N_u^i = 2$ is illustrated in Fig. 2. Initially, users are associated to each attocell, hence, we denote by U_{ik} the intended message for the k^{th} user in the i^{th} attocell, $\forall i = 1, \ldots, N_c$, $\forall k = 1, \ldots, N_u^i$. Similar to the single cell scenario, message U_{ik} is divided into a common part, U_{ik}^c, and a private part, U_{ik}^k. The common messages of all users in the i^{th} attocell are combined and encoded as a common stream denoted by s_i^c, decodable by all users in the i^{th} attocell, whereas U_{ik}^k is encoded as a private stream s_i^k to be decoded only by the k^{th} user. Then, the linear precoder $\mathbf{P}_i = [\mathbf{p}_i^c, \mathbf{p}_i^1, \mathbf{p}_i^2, \ldots, \mathbf{p}_i^{N_u^i}] \in \mathbb{R}^{N_l \times (N_u^i+1)}$ is designed at each attocell and multiplied by the streams vector $\mathbf{s}_i = [s_i^c, s_i^1, \ldots, s_i^{N_u^i}]^T$. Finally, a DC bias vector $\mathbf{I}_i^{DC} = I^{DC} \times \mathbf{1}_{N_l \times 1} \in \mathbb{R}^{N_l \times 1}$ is added to the signal. Thus, the transmitted signal by the i^{th} attocell is expressed as

$$\mathbf{x}_i = \mathbf{P}_i \mathbf{s}_i + \mathbf{I}_i^{DC}, \ \forall i = 1, \ldots, N_c. \tag{16}$$

The received signal by the k^{th} user in the i^{th} attocell will be the collection of all the transmitted signals from all attocells, which is given by

$$y_{ik} = \varsigma\zeta\Big[\left(\mathbf{h}_{ik}^i\right)^T \mathbf{P}_i \, \mathbf{s}_i + \sum_{\substack{j=1 \\ j \neq i}}^{N_c} \left(\mathbf{h}_{ik}^j\right)^T \mathbf{P}_j \, \mathbf{s}_j \Big] + \varsigma\zeta \sum_{j=1}^{N_c} \mathbf{I}_j^{DC} + n_{ik}. \tag{17}$$

In this section, we design the precoders of different attocells based on MMSE linear precoding, which has superior performance, especially at low SNR regimes. Hence, the MSE associated with decoding the common and private streams at the k^{th} user in the i^{th} attocell is represented, respectively, as

$$E_{ik}^c = \mathbb{E}\left(\|\hat{s}_{ik}^c - s_i^c\|^2 \right), \tag{18}$$

and

$$E_i^k = \mathbb{E}\left(\left\|\hat{s}_i^k - s_i^k\right\|^2 \right). \tag{19}$$

It is recalled that the detection process at each user in the i^{th} attocell begins by decoding the common stream in the i^{th} attocell and extracting the intended information from it; then, each user decodes its intended private stream. Therefore, in order to mitigate ICI, we assume that there is a certain level of coordination between the attocells to design their precoders. In this work, we opt to use CB technique for the precoders design of the common and private streams aiming to minimize the sum-MSE across all attocells. Hence, we formulate the sum-MSE minimization problem for the RSMA with CB as

$$\min_{\substack{\mathbf{P}_i, E_i^c, \\ \alpha_i^k, \alpha_{ik}^c}} \quad \text{SMSE} = \sum_{i=1}^{N_c} E_i^c + \sum_{i=1}^{N_c} \sum_{k=1}^{N_u^i} E_i^k \tag{P2}$$

$$\text{s.t.} \quad E_{ik}^c \leq E_i^c, \ \forall k \in \{1, 2..., N_u^i\}, \forall i \in 1, ..., N_c \tag{P2.a}$$

$$L_1(\mathbf{p}_i^\ell) \leqslant \min\left(I^{DC} - I_{min}, I_{\max} - I^{DC}\right) \mathbf{1}_{N_l \times 1}, \tag{P2.b}$$

where $\alpha_i^k, \alpha_{ik}^c$ are the equalizers used for the detection of the private and common streams, respectively. Moreover, E_i^c is the MSE of the common stream in the i^{th} attocell, which is set to the worst case according to constraints (P2.a). The objective function in (P2) is non-convex in terms of all optimization variables, so its solution is not straightforward. Thus, similar to the previous section, we opt to use AO algorithm to converge to a local sum-MSE solution, where the algorithm iterates between updating the precoders and the equalizer gains in order to converge. Next, we analyze the performance of the

TABLE I
SIMULATION PARAMETERS.

Parameter	Symbol	Value
Number of LED chips per array	N_b	3600 (60×60)
LED semi-angle at half power	$\varphi_{1/2}$	70^o
PD area	A	1 cm^2
Refractive index of PD	n	1.5
Gain of optical filter	$T_s(\phi)$	1
FoV of PD	ϕ_c	60^o
Maximum allowable current	$I_{\max}$	600 mA
Minimum allowable current	$I_{\min}$	400 mA
DC current	I^{DC}	500 mA
Bandwidth	B	20 MHz

TABLE II
USERS' LOCATIONS (N_u^i=2).

	Cell 1	Cell 2
Scenario I	User 1: [2.5,1.25,0.85]	User 3: [-2.5,1.25,0.85]
	User 2: [2.5,-1.25,0.85]	User 4: [-2.5,-1.25,0.85]
Scenario II	User 1: [1,2,0.85]	User 3: [-1,2,0.85]
	User 2: [1,-2,0.85]	User 4: [-1,-2,0.85]
Scenario III	User 1: [0.25,1.25,0.85]	User 3: [-0.25,1.25,0.85]
	User 2: [0.25,-1.25,0.85]	User 4: [-0.25,-1.25,0.85]

TABLE III
LED ARRAYS LOCATIONS FOR MULTI-CELL CONFIGURATION.

Cell 1	Cell 2
LED array 1: [2.5,1.25,3]	LED array 3: [-2.5,1.25,3]
LED array 2: [2.5,-1.25,3]	LED array 4: [-2.5,-1.25,3]

proposed system model in terms of the overall SE and EE, which are defined as [26]

$$\eta_{SE} = \frac{1}{B}\sum_{i=1}^{N_c}\sum_{k=1}^{N_u^i} R_{ik} \tag{21}$$

and

$$\eta_{EE} = \frac{1}{BP_T}\sum_{i=1}^{N_c}\sum_{k=1}^{N_u^i} R_{ik}, \tag{22}$$

where $P_T = N_b^2 \sum_{i=1}^{N_c} \mathbb{E}\left(\|\mathbf{x}_i\|^2\right)$ denotes the total power consumption of the system [37].

IV. Simulation Results

In this section we investigate the performance of the proposed RSMA with CB in terms of the SE and EE for a simple multi-cell configuration. In this context, we consider a room of size $10 \times 5 \times 3$ m^3 consisting of two attocells, each serving two users located within its coverage area. Based on this, we then compare its performance with that of the CB SDMA counterpart. To this end, we assume that the LED arrays in different cells are connected through backbone links in order to provide a certain level of coordination between them. Also, without loss of generality, we assume that $\varsigma = 1$ W/A, $\zeta = 1$ A/W. Furthermore, we assume the same optical devices characteristics as in [14]. For convenience, all parameters used are depicted in Table I.

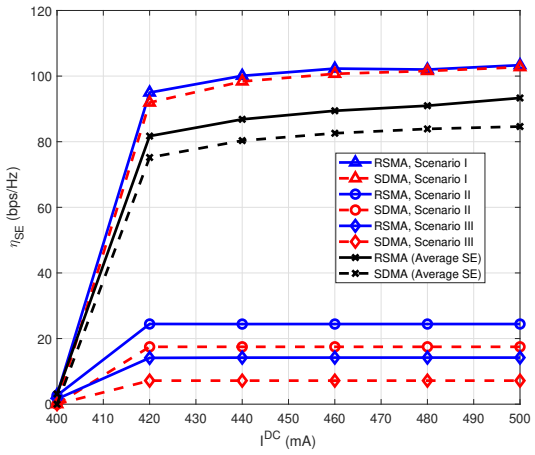

Fig. 3. SE versus DC current for different considered scenarios in multi-cell configuration.

To study the impact of different users' locations within an indoor space, we consider different scenarios, summarized in Table II, whereas the locations of the LED arrays in each attocell are depicted in Table III.

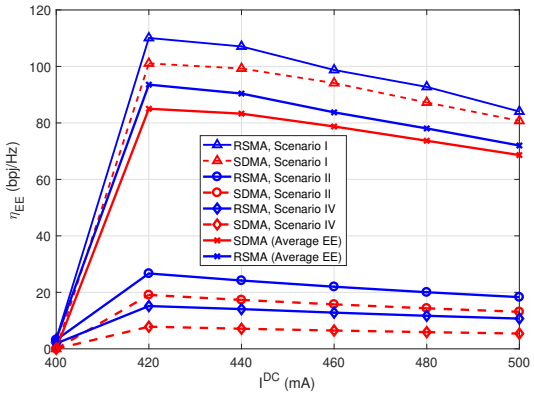

Fig. 4. EE versus DC current for different considered scenarios in multi-cell configuration.

Fig. 3 illustrates the SE performance of RSMA and SDMA for different scenarios. Specifically, in "scenario I" all users are located in the cells centers, whereas in "scenario II", all users are close to the boundary of the overlapped area between the two considered cells. Finally, in "scenario III" all users are located inside the overlapped area. It is evident that as I^{DC} increases, SE improves rapidly up to $I^{DC} = 420$ mA; then, it reached gradually its maximum value at $I^{DC} = 500$ mA. However, for scenarios where users experience high ICI, the SE saturates quickly. Finally, CB RSMA outperforms CB SDMA in terms of average SE. Additionally, Fig. 4 illustrates the EE performance of the proposed system model and SDMA with CB as a function of the DC bias. For all considered scenarios, as I^{DC} increases up-to 420 mA, the EE is enhanced due to the achieved high SE compared to power consumption. As the DC current exceeds 420 mA, the EE begins to decrease because more power is consumed in this region; yet, a small additional SE gain is still achieved. Moreover, it is evident that RSMA with CB exhibits a more prominent EE performance compared to SDMA with CB across all scenarios. Thus, RSMA proves more spectrally and energy-efficient than SDMA with CB in multi-cell VLC configurations due to its interference mitigation capabilities.

V. Conclusion

In the present work, we investigated rate-splitting multiple access for multiple-input single-output (MISO) VLC systems, taking into consideration the per-LED power constraints. We first presented background information about RSMA in single-cell MISO VLC systems, wherein the SINR and WSR expressions were explained for a two-user scenario. Subsequently, WSR optimization problem was discussed in order to design the precoders for the common and private streams. Then, in order to provide ubiquitous indoor coverage and to address user mobility issues in large indoor environments, we proposed RSMA in multi-cell VLC environments. Also, in order to enhance the performance of cell-edge VLC users, we utilized

coordinated beamforming for the precoders design, aiming to reduce the sum-MSE of the system. Through extensive simulations, we demonstrated the efficiency of our proposed RSMA models compared to the conventional SDMA technique with coordinated beamforming in terms of the achievable spectral and the energy efficiency for simple two-cell configuration.

ACKNOWLEDGMENT

This work was supported by Khalifa University Grants KU/FSU-8474000122 and KU/RC1-C2PS-T2/8474000137.

REFERENCES

[1] L. Grobe, A. Paraskevopoulos, J. Hilt, D. Schulz, F. Lassak, F. Hartlieb, C. Kottke, V. Jungnickel, and K. Langer, "High-speed visible light communication systems," *IEEE Commun. Mag.*, vol. 51, no. 12, pp. 60–66, Dec. 2013.

[2] Z. Ghassemlooy, W. Popoola, and S. Rajbhandari, *Optical Wireless Communications: System and Channel Modelling with MATLAB*, 2nd ed. CRC Press, May 2019.

[3] A. R. Ndjiongue, T. M. N. Ngatched, O. A. Dobre, and A. G. Armada, "VLC-based networking: feasibility and challenges," *IEEE Network*, vol. 34, no. 4, pp. 158–165, July/August 2020.

[4] H. Marshoud, S. Muhaidat, P. C. Sofotasios, M. Imran, B. S. Sharif, and G. K. Karagiannidis, "Optical asymmetric modulation for vlc systems - invited paper," in *2018 IEEE 87th Vehicular Technology Conference (VTC Spring)*, 2018, pp. 1–5.

[5] H. Marshoud, S. Muhaidat, P. C. Sofotasios, S. Hussain, M. A. Imran, and B. S. Sharif, "Optical non-orthogonal multiple access for visible light communication," *IEEE Wireless Communications*, vol. 25, no. 2, pp. 82–88, 2018.

[6] H. Marshoud, P. C. Sofotasios, S. Muhaidat, G. K. Karagiannidis, and B. S. Sharif, "On the performance of visible light communication systems with non-orthogonal multiple access," *IEEE Transactions on Wireless Communications*, vol. 16, no. 10, pp. 6350–6364, 2017.

[7] A. M. Aljaberi, S. A. Naser, P. C. Sofotasios, and S. Muhaidat, "Space shift keying modulation in non-orthogonal multiple access hybrid visible light communication systems (invited paper)," in *2020 3rd International Conference on Advanced Communication Technologies and Networking (CommNet)*, 2020, pp. 1–5.

[8] A. Aliaberi, P. C. Sofotasios, and S. Muhaidat, "Modulation schemes for visible light communications," in *2019 International Conference on Advanced Communication Technologies and Networking (CommNet)*, 2019, pp. 1–10.

[9] S. S. Bawazir, P. C. Sofotasios, S. Muhaidat, Y. Al-Hammadi, and G. K. Karagiannidis, "Multiple access for visible light communications: Research challenges and future trends," *IEEE Access*, vol. 6, pp. 26 167–26 174, 2018.

[10] H. Marshoud, P. C. Sofotasios, S. Muhaidat, and G. K. Karagiannidis, "Multi-user techniques in visible light communications: A survey," in *2016 International Conference on Advanced Communication Systems and Information Security (ACOSIS)*, 2016, pp. 1–6.

[11] H. Marshoud, P. C. Sofotasios, S. Muhaidat, B. S. Sharif, and G. K. Karagiannidis, "Optical adaptive precoding for visible light communications," *IEEE Access*, vol. 6, pp. 22 121–22 130, 2018.

[12] A. Jovicic, J. Li, and T. Richardson, "Visible light communication: Opportunities, challenges and the path to market," *IEEE Commun. Mag.*, vol. 51, no. 12, pp. 26–32, Dec. 2013.

[13] H. S. Hussein and M. Hagag, "Optical MIMO-OFDM with fully generalized index-spatial LED modulation," *IEEE Commun. Lett.*, vol. 23, no. 9, pp. 1556–1559, Sep. 2019.

[14] S. Naser, P. C. Sofotasios, L. Bariah, W. Jaafar, S. Muhaidat, M. Al-Qutayri, and O. A. Dobre, "Rate-splitting multiple access: Unifying NOMA and SDMA in MISO VLC channels," *IEEE Open Journal of Vehicular Technology*, vol. 1, pp. 393–413, 2020.

[15] S. A. Naser and P. C. Sofotasios, "Generalization of space-time block coded-spatial modulation for high data rate VLC systems (invited paper)," in *2020 3rd International Conference on Advanced Communication Technologies and Networking (CommNet)*, 2020, pp. 1–5.

[16] F. Ahmed, A. A. Dowhuszko, and O. Tirkkonen, "Self-organizing algorithms for interference coordination in small cell networks," *IEEE Trans. Veh. Technol.*, vol. 66, no. 9, pp. 8333–8346, Sept. 2017.

[17] M. Kashef, M. Abdallah, K. Qaraqe, H. Haas, and M. Uysal, "Coordinated interference management for visible light communication systems," *IEEE J. Opt. Commun. Netw.*, vol. 7, no. 11, pp. 1098–1108, Nov. 2015.

[18] R. Bai, H. Tian, B. Fan, and S. Liang, "Coordinated transmission based interference mitigation in VLC network," in *Proc. IEEE 82nd Vehicular Technology Conference (VTC2015-Fall)*, 2015, pp. 1–5.

[19] K. Zhou, C. Gong, and Z. Xu, "Color planning and intercell interference coordination for multicolor visible light communication networks," *J. Lightw. Technol.*, vol. 35, no. 22, pp. 4980–4993, Nov. 2017.

[20] S. Jung, D. Kwon, S. Yang, and S. Han, "Reduction of inter-cell interference in asynchronous multi-cellular VLC by using OFDMA-based cell partitioning," in *Proc. 18th International Conference on Transparent Optical Networks (ICTON)*, 2016, pp. 1–4.

[21] C. Chen, W. Zhong, H. Yang, S. Zhang, and P. Du, "Reduction of SINR fluctuation in indoor multi-cell VLC systems using optimized angle diversity receiver," *J. Lightw. Technol.*, vol. 36, no. 17, pp. 3603–3610, Sept. 2018.

[22] H. Ryoo, D. Kwon, S. Yang, and S. Han, "Differential optical detection in VLC for inter-cell interference reduced flexible cell planning," *IEEE Photon. Technol. Lett.*, vol. 28, no. 23, pp. 2728–2731, Dec. 2016.

[23] T. V. Pham and A. T. Pham, "Coordination/cooperation strategies and optimal zero-forcing precoding design for multi-user multi-cell VLC networks," *IEEE Trans. Commun.*, vol. 67, no. 6, pp. 4240–4251, Jun. 2019.

[24] H. Yang, C. Chen, W. Zhong, and A. Alphones, "Joint precoder and equalizer design for multi-user multi-cell MIMO VLC systems," *IEEE Trans. Veh. Technol.*, vol. 67, no. 12, pp. 11 354–11 364, Dec. 2018.

[25] X. Zhang, Q. Gao, C. Gong, and Z. Xu, "User grouping and power allocation for NOMA visible light communication multi-cell networks," *IEEE Commun. Lett.*, vol. 21, no. 4, pp. 777–780, Apr. 2017.

[26] S. Tao, H. Yu, Q. Li, and Y. Tang, "Strategic analysis of user association based on power-domain non-orthogonal multiple access in visible light communication multi-cell networks," in *Proc. IEEE 19th Int. Conf. Commun. Technol. (ICCT)*, 2019, pp. 710–714.

[27] J. Shi, J. He, K. Wu, and J. Ma, "Enhanced performance of asynchronous multi-cell VLC system using OQAM/OFDM-NOMA," *J. Lightw. Technol.*, vol. 37, no. 20, pp. 5212–5220, Oct. 2019.

[28] M. W. Eltokhey, M. A. Khalighi, A. S. Ghazy, and S. Hranilovic, "Hybrid NOMA and ZF pre-coding transmission for multi-cell VLC networks," *IEEE Open J. Commun. Soc.*, vol. 1, pp. 513–526, Apr. 2020.

[29] M. W. Eltokhey, M. A. Khalighi, and Z. Ghassemlooy, "Dimming-aware interference mitigation for NOMA-based multi-cell VLC networks," *IEEE Commun. Lett.*, pp. 1–1, Jul. 2020.

[30] L. Yin and B. Clerckx, "Rate-splitting multiple access for multigroup multicast and multibeam satellite systems," *IEEE Trans. Commun.*, pp. 1–1, 2020.

[31] Y. Mao and B. Clerckx, "Beyond dirty paper coding for multi-antenna broadcast channel with partial CSIT: A rate-splitting approach," *IEEE Trans. Commun.*, vol. 68, no. 11, pp. 6775–6791, 2020.

[32] O. Dizdar, Y. Mao, W. Han, and B. Clerckx, "Rate-splitting multiple access: A new frontier for the PHY layer of 6G," *arXiv*, vol. abs/2006.01437, 2020.

[33] Y. Mao, B. Clerckx, and V. Li, "Rate-splitting multiple access for downlink communication systems: Bridging, generalizing, and outperforming SDMA and NOMA," *EURASIP J. Wireless Commun. and Network.*, no. 133, pp. 1–54, May 2018.

[34] Y. Mao, B. Clerckx, and V. O. K. Li, "Energy efficiency of rate-splitting multiple access, and performance benefits over SDMA and NOMA," in *2018 15th International Symposium on Wireless Communication Systems (ISWCS)*, 2018, pp. 1–5.

[35] T. Komine and M. Nakagawa, "Fundamental analysis for visible-light communication system using LED lights," *IEEE Trans. Consum. Electron.*, vol. 50, no. 1, pp. 100–107, Feb. 2004.

[36] S. S. Christensen, R. Agarwal, E. De Carvalho, and J. M. Cioffi, "Weighted sum-rate maximization using weighted MMSE for MIMO-BC beamforming design," *IEEE Trans. Wireless Commun.*, vol. 7, no. 12, pp. 4792–4799, Dec. 2008.

[37] Y. Hsiao, Y. Wu, and C. Lin, "Energy-efficient beamforming design for MU-MISO mixed RF/VLC heterogeneous wireless networks," *IEEE Trans. Sig. Process.*, vol. 67, no. 14, pp. 3770–3784, Jul. 2019.